On the Mechanism of Gating Charge Movement of ClC-5, a Human Cl^-/H^+ Antiporter

Giovanni Zifarelli, Silvia De Stefano, Ilaria Zanardi, and Michael Pusch*
Istituto di Biofisica, The National Research Council, Genoa, Italy

ABSTRACT ClC-5 is a Cl^-/H^+ antiporter that functions in endosomes and is important for endocytosis in the proximal tubule. The mechanism of transport coupling and voltage dependence in ClC-5 is unclear. Recently, a transport-deficient ClC-5 mutant (E268A) was shown to exhibit transient capacitive currents. Here, we studied the external and internal Cl^- and pH dependence of the currents of E268A. Transient currents were almost completely independent of the intracellular pH. Even though the transient currents are modulated by extracellular pH, we could exclude that they are generated by proton-binding/unbinding reactions. In contrast, the charge movement showed a nontrivial dependence on external chloride, strongly supporting a model in which the movement of an intrinsic gating charge is followed by the voltage-dependent low-affinity binding of extracellular chloride ions. Mutation of the external Glu-211 (a residue implicated in the coupling of Cl^- and proton transport) to aspartate abolished steady-state transport, but revealed transient currents that were shifted by ~150 mV to negative voltages compared to E268A. This identifies Glu_{ext} as a major component of the gating charge underlying the transient currents of the electrogenic ClC-5 transporter. The molecular events underlying the transient currents of ClC-5 emerging from these results can be explained by an inward movement of the side chain of Glu_{ext}, followed by the binding of extracellular Cl^- ions.

INTRODUCTION

Anion-transporting CLC proteins are found in all phyla (1). Interestingly, some CLCs are passive Cl^- channels, like the Torpedo ClC-0 (2,3), whereas others are secondary active anion/proton antiporters with a two-anion:one-proton stoichiometry (4–10). In humans, four of the nine CLC genes code for Cl^- channels that function in the plasma membrane, whereas the remaining five are Cl^-/H^+ antiporters found mostly in endosomal and lysosomal membranes (11). Studies with knock-in mice carrying uncoupling mutations have shown that the antiport activity of these intracellular CLCs is physiologically relevant and cannot be substituted by a passive Cl^- conductive transport mechanism (12,13). Genetic defects of the endosomal Cl^-/H^+ antiporter ClC-5 lead to Dent's disease (14), caused by impaired endocytosis in the kidney proximal tubule (15–18).

Like most CLC channels and transporters, ClC-5 is voltage-dependent (19). However, unlike voltage-gated cation channels, in which a specialized voltage-sensor domain mechanically couples the membrane electrical field to pore opening (20), the mechanism of voltage sensitivity has proved much more elusive for the voltage-sensitive CLC proteins (11,21). The crystal structure of the CLC antiporter from *Escherichia coli*, ClC-ec1 (4,22,23), describes a molecular architecture that is very similar for both CLC channels and transporters and does not show any cluster of charged residue that could act as a voltage sensor in a manner similar to K^+ channels. The structure revealed a buried, central Cl^- binding site S_{cen} and an internal, solution-exposed site S_{int}. In addition, a conserved glutamate residue, the gating glutamate or Glu_{ext} (E211 in ClC-5) (24), is a central element in all CLC exchangers studied so far. During the transport cycle, the negatively charged side chain of Glu_{ext} is protonated and displaced, probably toward the extracellular vestibule, giving way for the binding of a third Cl^- ion at S_{ext}, very close to S_{cen} (Fig. 1) (23). Recently, the structure of a eukaryotic CLC revealed that the glutamate side chain can also bend toward the internal side and occupy the central site (25) (Fig. 1). Whereas protons and Cl^- ions utilize the same pathway from Glu_{ext} to the extracellular (luminal) solution, the two substrates take different routes from Glu_{ext} to the inside.

Mutagenesis studies have indicated the proton glutamate (E268 in ClC-5) as a candidate to be the intracellular entry/exit point for protons (26). Mutating the proton glutamate to Ala in ClC-ec1 abolishes H^+ transport and renders the transporter a passive Cl^- conductance (26), similar to mutating the gating glutamate (4). Surprisingly, the corresponding mutation in ClC-5 (E268A) inhibits steady-state transport (24), but Smith and Lippiat (27) have recently reported that the mutant E268A exhibits transient currents upon voltage steps to large positive voltages. These transient currents may offer the possibility to glean information on the molecular details of transport coupling in ClC-5. Here we studied the dependence of the transient currents on the extracellular and intracellular pH and Cl^- concentration. We conclude that the transient currents represent the movement of an intrinsic gating charge followed by the voltage-dependent binding of extracellular Cl^- ions. In addition, we find that the gating glutamate mutation E211D abolishes stationary transport but displays transient currents that are shifted by ~150 mV compared to the proton glutamate

Submitted January 13, 2012, and accepted for publication March 29, 2012.

*Correspondence: pusch@ge.ibf.cnr.it

Editor: Jose Faraldo-Gomez.

0006-3495/12/05/2060/10 $2.00

doi: 10.1016/j.bpj.2012.03.067

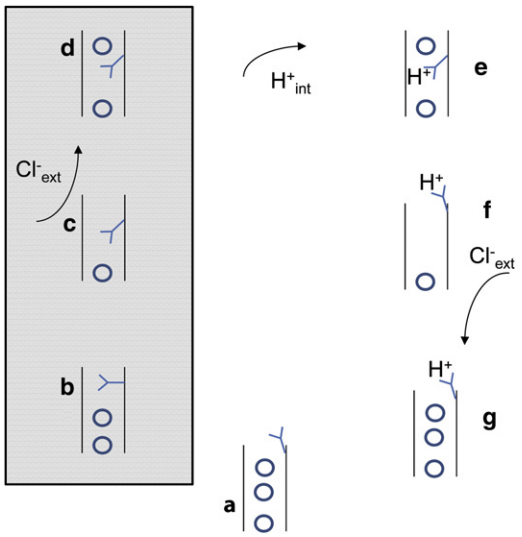

FIGURE 1 Schematic model of the transport cycle of ClC-5. The hypothetical model is based on the one suggested by Feng et al. (25) for CmClC with the addition of state *c*. (*Circles* represent Cl^- ions; *shaded box* represents the branch of the transport cycle that is accessible to the E268A mutant.) In state *a*, the side chain of E211 is unprotonated and the transporter has all the binding sites occupied by Cl^- ions. In state *b*, the side chain of E211 moves to occupy S_{ext} and one Cl^- ion moves intracellularly. In state *c*, the side chain of E211 moves to occupy S_{cen} and this is associated with the transport of another Cl^- ion whereas S_{ext} is transiently empty but binds an extracellular Cl^- ion in state *d*. From this conformation E211 can be protonated by an intracellular proton (state *e*) and can move outwardly (state *f*), giving way to Cl^- binding from the extracellular space (state *g*). The model is not intended to provide a realistic description of the ClC-5 transport cycle, but rather to guide a mechanistic interpretation of the results.

mutation, identifying E211 as a major component underlying the transient currents.

MATERIALS AND METHODS

Molecular biology and transient expression

Human ClC-5 and mutants were in the PTLN vector for expression in oocytes and in a pcDNA3-derived vector for expression in HEK293 cells (5). Mutants were generated by polymerase-chain reaction and sequenced. Expression in *Xenopus* oocytes and two electrode voltage-clamp recording conditions were essentially performed as described earlier (24). Transient transfection of HEK293 cells was performed using the Effectene kit (Qiagen, Milan, Italy), a lipid carrier method of DNA transfection. Cells were cotransfected with CD8 and positively transfected cells were visualized using anti-CD-antibody-coated microbeads 2–3 days after transfection (28). Standard whole-cell patch-clamp recording (29) was performed with pipettes pulled from borosilicate capillaries (Hilgenberg, Malsfeld, Germany). Currents were recorded using an Axopatch 200A (Axon Instruments, Foster City, CA) amplifier using a custom acquisition program (GePulse; freely available at http://www.ge.ibf.cnr.it/~pusch.ibf/programs-mik.htm).

Solutions

For two-electrode voltage-clamp recordings, the standard extracellular solution contained 100 mM NaCl, 5 mM $MgSO_4$, 10 mM HEPES, pH 7.3. Chloride was reduced by substitution of NaCl with NaGlutamate. For patch-clamp recordings, the standard intracellular solution contained 130 mM CsCl, 2 mM $MgSO_4$, 1 mM EGTA, and 10 mM HEPES, pH 7.3. The standard extracellular solution contained 140 mM CsCl, 5 mM $MgSO_4$, and 10 mM HEPES, pH 7.3. Chloride was reduced in these solutions by substitution of CsCl with CsGlutamate. For solutions with different pH values, HEPES was replaced by Mes for pH $<$ 6.3 and by CAPS for pH $>$ 8.3.

Pulse protocols

For wild-type (WT), E268A at all pH values and for E211D at pH_{ext} 5.3, the pulse protocol consisted of voltage steps of 10 ms from 200 to −100 mV with 10 mV decrements from a holding potential of 0 mV. For E211D at pH_{ext} 6.3–9, the voltage steps were from 120 to −120 mV and were preceded by a 10-ms conditioning prepulse to −120 mV. Linear capacitive and leak currents were estimated by applying several pulses in a voltage range in which the $Q(V)$ relationship was essentially flat, and subtracting the appropriately scaled response from the main pulses (similar but not identical to the classical P/−n protocol). For WT and E268A, the holding potential of the P/−n pulses was 0 mV or −60 mV. For E211D and E211D/E268A, the holding potential of the P/−n pulses was set to +40 mV. Sampling frequency in patch-clamp experiments was between 100 and 200 kHz after filtering at 30–50 kHz using the built-in filter of the amplifier.

Analysis

Raw data were analyzed using a custom analysis program (Ana; freely available at http://www.ge.ibf.cnr.it/~pusch.ibf/programs-mik.htm). Steady-state charge-voltage relationships were constructed by integrating the current responses at a constant tail-voltage that followed the activating voltage steps (see, e.g., Fig. 2). The kinetics of the currents measured with the two-electrode voltage-clamp are limited by the filtering effect of the oocyte capacitance and clearly do not reflect the true kinetics of the process.

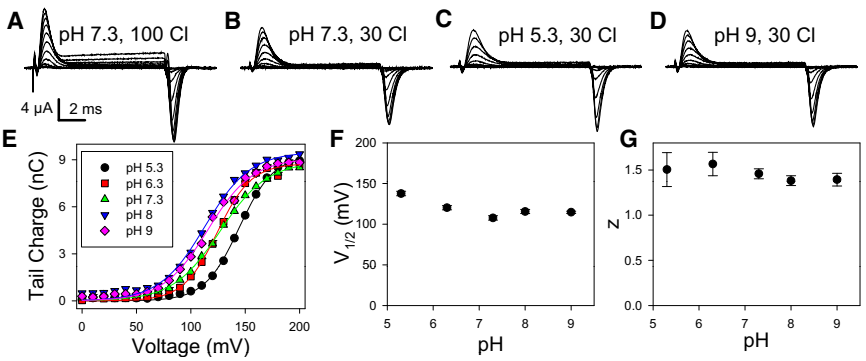

FIGURE 2 Transient currents of E268A are independent of pH_{ext}. (*A–D*) Voltage-clamp recordings from one oocyte at the indicated conditions of pH and $[Cl^-]_{ext}$. (*E*) Representative $Q(V)$-curves measured from the response at the negative tail potential (obtained for one oocyte) (*symbols*) together with fits of Eq. 1 (*lines*) at the indicated pH values (at 30 mM $[Cl^-]_{ext}$). Average values are shown for $V_{1/2}$ (*F*) and the apparent gating valence, z (*G*), as a function of pH measured at 30 mM $[Cl^-]_{ext}$. Error bars indicate mean ± SE ($n \geq 9$).

Nevertheless, the two-electrode voltage-clamp allows the determination of the charge related to the transient currents. Figures were prepared using SigmaPlot (Systat Software, Chicago, IL).

RESULTS

Modulation of transient currents by extracellular pH

We expressed ClC-5-E268A in *Xenopus* oocytes as well as in HEK cells and assayed currents using the two-electrode voltage-clamp and the patch-clamp technique, respectively. In agreement with Smith and Lippiat (27), we observed large transient outward currents upon stepping the voltage to positive voltages and negative transient currents upon stepping back to the holding potential (Fig. 2, *A–D*). The relatively small steady-state outward currents seen in the oocytes at positive voltages (Fig. 2 *A*) are most likely due to endogenous currents, as similar currents were seen in noninjected oocytes (see Fig. S7 *F* in the Supporting Material), but they almost vanished at lower $[Cl^-]_{ext}$ (Fig. 2 *B*). Thus, we tested the effect of pH_{ext} at 30 mM $[Cl^-]_{ext}$. Charge voltage-relationships, $Q(V)$, were constructed by integrating the currents at the tail voltage as a function of the prepulse voltage (Fig. 2 *E*). The $Q(V)$ was fitted with a Boltzmann function of the form

$$Q(V) = \frac{Q_{max}}{1 + e^{z\left(V_{1/2} - V\right)F/(RT)}}, \quad (1)$$

where z is the apparent gating valence of the process, $V_{1/2}$ the voltage of half-maximal activation, and F, R, and T represent the Faraday constant, the gas constant, and the absolute temperature, respectively (*line*s in Fig. 2 *E*). Varying pH_{ext} from 5.3 to 9 had only relatively small effects on the transient currents (Fig. 2, *B–D*) and on the resulting values of $V_{1/2}$ and z (Fig. 2, *F* and *G*). Thus, although the transient currents are clearly modulated by external pH, it can be excluded that proton-binding/unbinding reactions underlie the transient currents. Otherwise, we would expect a gradual reduction of the inward transient currents upon lowering the proton concentration from 0.1 μM (pH 7) to 1 nM (pH 9). In particular, upon lowering the proton concentration, one would also expect a shift of the Q-V relationship to more positive voltages, opposite to the observed shift.

Transient currents are not carried by movement of intracellular protons

The whole-cell patch-clamp method offers the possibility to test the effect of intracellular parameters. We applied this method to test the hypothesis that the transient outward currents of the E268A mutant are associated with the translocation of protons from the intracellular side toward the external side of the transporter. According to this hypothesis, transient currents should decrease if $[H^+]_{int}$ is significantly reduced. We thus performed experiments with an intracellular solution at pH 9, i.e., at low $[H^+]_{int}$ (see Fig. S1). Transient currents were recorded immediately after establishing the whole-cell configuration and followed during the perfusion of the cytosol with the pipette solution (see Fig. S1 *B*). Even though free proton diffusion is fast, the equilibration of the pH between the patch pipette and the cytosol depends on the diffusion of cytosolic and pipette buffers and full equilibration can be expected to occur within roughly 1–3 min (30). No significant change of the transient currents was observed for >3 min after break-in (see Fig. S1 *C*) and only a very small effect on the $Q(V)$ was seen (see Fig. S1 *D*). Thus, the outward transient currents are unlikely to reflect the translocation of protons from the cytosol into the transporter.

Dependence of transient currents on extracellular chloride

Smith and Lippiat (27) have reported that extracellular Cl^- modifies the transient currents mediated by E268A, but concluded that Cl^- is not directly involved in their generation. Here, we studied the dependence on $[Cl^-]_{ext}$ in a quantitative manner to gain insight into the mechanism underlying the transient currents. Fig. 3, *A–D*, show recordings from one oocyte at various $[Cl^-]_{ext}$ and in Fig. 3 *E* the corresponding $Q(V)$s are plotted together with fits of a

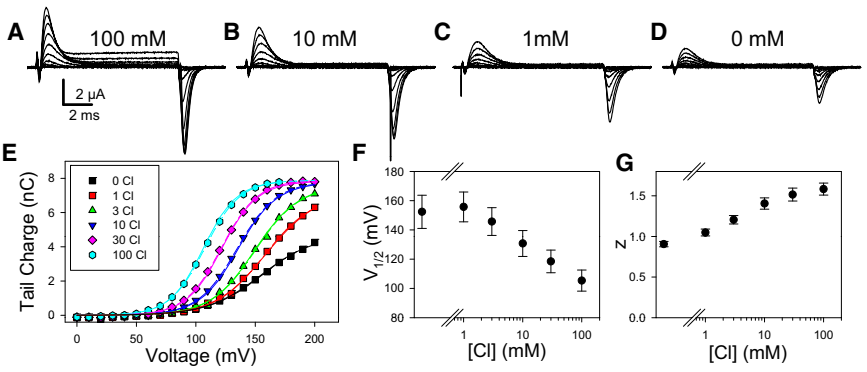

FIGURE 3 Extracellular chloride dependence of the transient currents of E268A. (*A–D*) Voltage-clamp recordings from one oocyte at the indicated $[Cl^-]_{ext}$. (*E*) $Q(V)$-relationships of this oocyte are superimposed with fits of Eq. 1 (*dashed lines*) and the predictions of the charge-voltage relationship for model III (Eq. 2) (*solid lines*; note that *dashed lines* and *solid lines* largely overlap). For the 0-Cl data, a contaminating concentration of 80 μM was assumed (see Fig. S3 in the Supporting Material). Average values are shown for $V_{1/2}$ (*F*) and the apparent gating valence, z (*G*), as a function of $[Cl^-]_{ext}$. Error bars indicate mean ± SE ($n \geq 4$).

Boltzmann function as described above (*dashed lines* in Fig. 3 *E*).

Reducing $[Cl^-]_{ext}$ progressively shifts the $Q(V)$ to more positive values and reduces the maximal gating charge obtained at 200 mV. Average values of the voltage of half-maximal activation, $V_{1/2}$, and the apparent gating valence, z, are shown in Fig. 3, parts *F* and *G*, respectively, as a function of $[Cl^-]_{ext}$.

Possible mechanisms that explain the chloride dependence

In a most simple model, voltage-dependent binding of Cl^- ions directly underlies the transient currents according to Model I,

$$U \underset{k_{off}(V)}{\overset{k_{on}(V)[Cl^-]_{ext}}{\rightleftarrows}} B.$$

State U represents the unbound transporter and state B the transporter in which Cl^- is bound with a voltage-dependent dissociation constant $K_D(V) = k_{off}/k_{on} = K_D(0)\exp(-z_K\varphi)$, where $\varphi = V\,F/(RT)$. However, the model does not provide an adequate fit of the steady-state data as illustrated in Fig. S2 *A*.

In a slightly more complicated model, voltage-dependent binding of chloride is a prerequisite for a following conformational change as Model II,

$$U \underset{k_{off}(V)}{\overset{k_{on}(V)[Cl^-]_{ext}}{\rightleftarrows}} B \underset{\beta}{\overset{\alpha}{\rightleftarrows}} B^*,$$

in which U represents the unbound transporter to which Cl^- binds in a voltage-dependent manner and states B and B^* are connected by voltage-dependent rate constants $\alpha(V) = \alpha_0 \exp(z_a\varphi)$ and $\beta(V) = \beta_0\exp(-z_\beta\varphi)$, where α_0 and β_0 are the respective rate constants at 0 mV, z_α and z_β, the respective gating valences.

To calculate the prediction of Model II for the $Q(V)$ relationship, we consider that state B differs from state U by z_K elementary charges and state B^* carries an additional charge with a valence of $z_C = z_\alpha + z_\beta$. Thus, for Model II the charge voltage-relationship can be calculated by $Q(V) \sim z_K\,p(B) + (z_K + z_C)p(B^*)$, where $p(B)$ is the probability to be in state B and $p(B^*)$ is the probability to be in state B^*. As illustrated in Fig. S2 *B*, however, Model II did not provide an adequate fit of the steady-state data.

Alternatively, a conformational change could be followed by a voltage-dependent chloride-binding step as detailed in Model III,

$$U \underset{\beta}{\overset{\alpha}{\rightleftarrows}} U^* \underset{k_{off}(V)}{\overset{k_{on}(V)[Cl^-]_{ext}}{\rightleftarrows}} B.$$

For Model III, $Q(V) \sim z_C\,p(U^*) + (z_K + z_C)p(B)$, thus predicting a $Q(V)$ relationship of the form

$$Q(V) = Q_{max}\frac{1 + \frac{z_C}{z_K + z_C}\frac{K_D(0)e^{-z_K\varphi}}{[Cl]}}{1 + \frac{K_D(0)e^{-z_K\varphi}}{[Cl]} + \frac{K_D(0)r_0e^{-(z_C+z_K)\varphi}}{[Cl]}}, \quad (2)$$

where $r_0 = \beta_0/\alpha_0$ is the ratio of the rate constants at 0 mV. Voltage dependence enters Eq. 2 only explicitly in the exponential terms containing the variable φ. A fit of Eq. 2 to the data set of Fig. 3 is shown as solid lines in Fig. 3 *E*. It can be seen that the $Q(V)$ relationships are qualitatively well described by this simple model. Average parameters obtained from four different cells are $z_C = 1.1 \pm 0.1$; $r_0 = \beta_0/\alpha_0 = 520 \pm 200$, $z_K = 0.85 \pm 0.07$; and $K_D(0) = 0.8 \pm 0.3$ M (mean ± SE). In the context of the model, approximately equal voltage dependence is assigned to the Cl^- binding step ($z_K \sim 0.85$) and to the conformational change ($z_C \sim 1.1$). Cl^- binding at 0 mV is of low affinity ($K_D(0\text{ mV}) = 0.8$ M), but because binding is voltage-dependent, $K_D(V) < 10$ mM for $V > 130$ mV.

A kinetic analysis of the transient currents would, in principle, allow us to test Model III more stringently and to assign values to the four rate constants. However, even in whole-cell recordings, the time course of the currents was too much influenced by the series resistance and cell capacitance, rendering a quantitative analysis unfeasible (data not shown).

Mutations of the gating glutamate alter transient currents

Neutralizing the gating glutamate E211 eliminates H^+ transport and renders ClC-5 a pure Cl^- conductance, even if combined with the proton glutamate mutation E268A (24). In addition, the E211A mutation also abolished transient currents (27). Also the double-mutant E211C/E268A, which similarly to E211A conducted Cl^- but not protons, did not display transient currents (see Fig. S4). However, because of the drastic alteration of the transport properties, from the absence of transient currents in the Glu_{ext} neutralizing mutants it cannot be safely concluded that Glu_{ext} itself represents the intrinsic mobile charge underlying the transient currents. Therefore, we assayed the conservative mutation E211D in which the alkyl chain that separates the carboxylate moiety from the peptide backbone is shorter by only one CH_2 group.

The mutant reduced steady-state current and proton transport below the limit of detection (see Fig. S5), but displayed clear transient currents (Fig. 4 *A*). Compared to E268A, the $Q(V)$ was dramatically shifted to more negative voltages (Fig. 4 *B*). For this reason, pulse protocols for E211D included a prepulse to −120 mV to fully deactivate the transient currents and hence obtain maximal charge movement during the following voltage steps. At difference with E268A, the transient currents of E211D at pH_{ext} 7.3 were

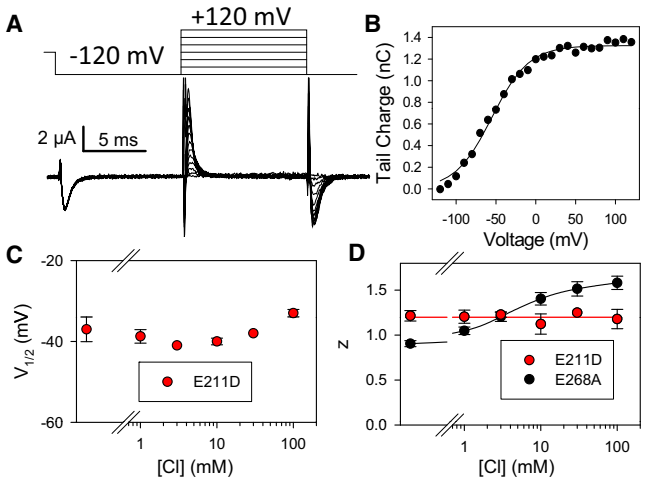

FIGURE 4 Extracellular chloride dependence of the transient currents of the mutant E211D at pH_{ext} 7.3. (*A*) Example current traces from an oocyte obtained using the pulse protocol shown. (*B*) *Q*(*V*)-relationships of this oocyte are superimposed with a fit of Eq. 1. Average values are shown for $V_{1/2}$ (*C*) and the apparent gating valence, *z* (*D*), as a function of $[Cl^-]_{ext}$. Error bars indicate mean ± SE ($n \geq 3$). (*D*) Values of mutant E268A from Fig. 2 *G* are additionally shown for comparison. The shaded line (*red line* in the *online version*) indicates the average for E211D; the solid (*black*) line connects points of E268A with a spline function.

almost completely independent of $[Cl^-]_{ext}$ (Fig. 4 *C*). The apparent gating charge was ~1.2, and also independent of $[Cl^-]_{ext}$ (Fig.4 *D*). The double-mutant E211D/E268A exhibited very similar properties as E211D, with a small left shift of the *Q*(*V*) relationship compared to the single mutant E211D (see Fig. S6).

The dependence on extracellular pH of E211D and E211D/E268A differs from the one of E268A

We additionally assessed the dependence of the transient currents of E211D and E211D/E268A on pH_{ext} (at 30 mM $[Cl^-]_{ext}$) (Fig. 5). The charge-voltage distribution for E211D and E211D/E268A is strongly affected by pH (Fig. 5 *D*). Compared to pH 7.3, the $V_{1/2}$ is shifted toward depolarized voltages by acidic pH changing by >100 mV between pH 7.3 and 5.3, whereas basic pH had only a minor effect (Fig. 5, *D* and *E*). On the other hand, the pH_{ext} has only a minor effect on *z*, with values close to 1 across the whole pH range tested (Fig. 5 *F*).

As for E268A, the nature of the pH dependence excludes that, for the E211D mutant, transient currents are generated by proton-binding/unbinding reactions: inward transient currents are not smaller at pH 9 than at pH 5.3 and the Q-V relationship is shifted to negative voltages upon lowering the extracellular proton concentration. We can only speculate about the molecular mechanism of the pH modulation. One possibility is that protonation of the aspartate residue in the mutants E211D and E211D/E268A increases its preference for an external binding site. This prompted us to investigate whether, at acidic pH, the transient currents of the two constructs might acquire a dependence on $[Cl^-]_{ext}$ similar to that of E268A. However, as illustrated in Fig. 6, the $V_{1/2}$ of the charge-voltage distribution at pH 5.3 is independent from $[Cl^-]_{ext}$ (for comparison, the figure also shows data points for E268A).

Importantly, the similar pH_{ext} dependence (Fig. 5) and $[Cl^-]_{ext}$ dependence at both pH_{ext} 7.3 and 5.3 (Fig. 4 and Fig. 6, respectively) of E211D and E211D/E268A strongly argues against a role of intracellular protons in regulating the conformational changes of the aspartate residue.

Transient currents of E211D depend on intracellular Cl^- similarly as those of E268A

Smith and Lippiat (27) showed that the transient currents of E268A are modulated by $[Cl^-]_{int}$ such that the *Q*(*V*) relationship is leftward-shifted at lower $[Cl^-]_{int}$. This suggests the hypothesis that the phenotype of the E211D mutant, which is also drastically leftward-shifted compared to E268A, could reflect a situation in which intracellular anions are no longer able to impede the charge translocation. We found, however, that the transient currents of E211D are affected by $[Cl^-]_{int}$ similar to the currents of E268A (Fig. 7): the voltage of half-maximal activation is ~15 mV

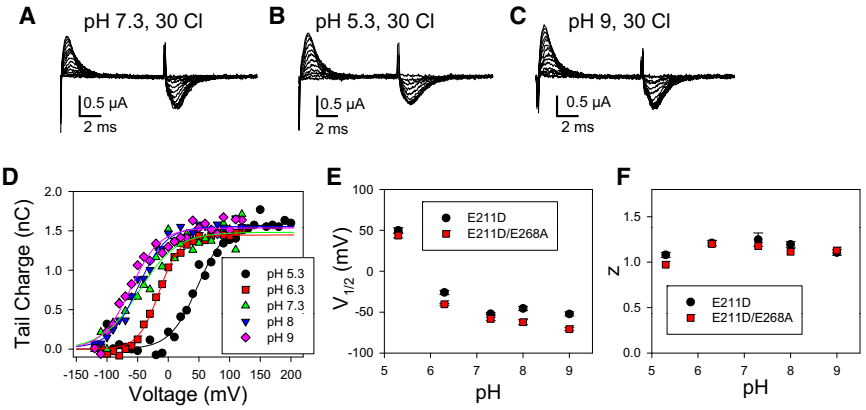

FIGURE 5 Dependence on extracellular pH of the transient currents of the mutants E211D and E211D/E268A. (*A–C*) Voltage-clamp recordings from one oocyte expressing E211D/E268A at the indicated conditions of pH and $[Cl^-]_{ext}$. (*D*) *Q*(*V*)-relationships of this oocyte are superimposed with fits of Eq. 1. Average values are shown for $V_{1/2}$ (*E*) and the apparent gating valence, *z* (*F*), as a function of pH_{ext}. Error bars indicate mean ± SE ($n \geq 3$).

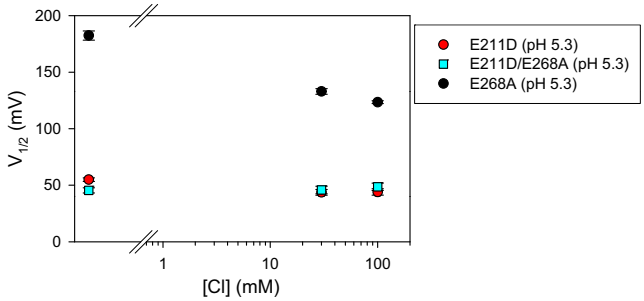

FIGURE 6 Extracellular chloride dependence of the mutants E211D, E268A, and E211D/E268A at pH_{ext} 5.3. Average values of $V_{1/2}$ obtained by fitting the $Q(V)$ relationship with Eq. 1. Error bars indicate mean ± SE ($n \geq 4$).

more negative in 30 mM $[Cl^-]_{int}$ compared to 130 mM $[Cl^-]_{int}$, a shift close to what we observe for E268A in the same conditions (Fig. 7 *B*).

Transient currents in WT ClC-5

WT ClC-5 shows transient currents in the range between 0 and 100 mM $[Cl^-]_{ext}$ (Fig. 8 and see Fig. S7). The transients become progressively smaller by decreasing $[Cl^-]_{ext}$ (Fig. 8 and see Fig. S7). However, noninjected oocytes, while showing only negligible transient currents at $[Cl^-]_{ext} \leq$ 30 mM, displayed in most cases unspecific transient currents

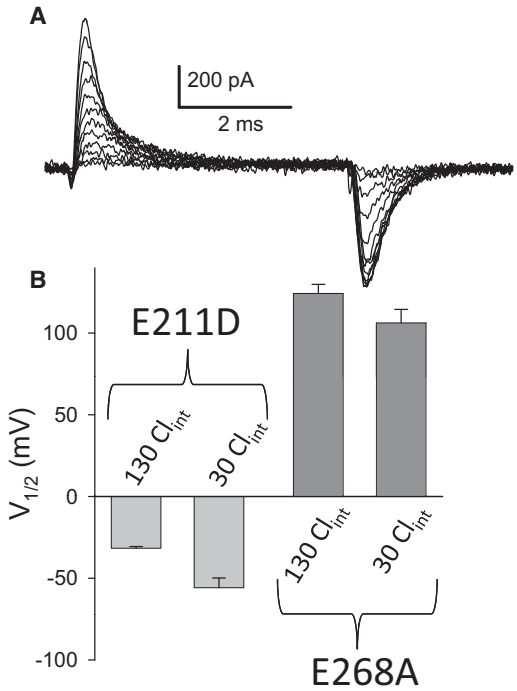

FIGURE 7 Dependence of transient currents on $[Cl^-]_{int}$. (*A*) Example current traces from a cell expressing mutant E211D obtained using a similar pulse protocol as shown in Fig. 4 *A*. (*B*) Average values of $V_{1/2}$ obtained from Boltzmann fits are shown for 130 mM $[Cl^-]_{int}$ and 30 mM $[Cl^-]_{int}$ for mutant E268A and mutant E211D, respectively.

at 100 mM $[Cl^-]_{ext}$ (see Fig. S7). These transients are not likely to perturb significantly the robust transients observed for WT ClC-5 at $[Cl^-]_{ext} \leq$ 30 mM (and for E268A and E211D). However, they precluded a quantitative analysis of the smaller transients observed in the WT at 100 mM Cl^-, that were therefore excluded from the analysis shown in Fig. 8. Fig. 8 *E* shows that the maximal charge, Q_{max}, estimated from the fit with Eq. 1 of the charge-voltage distribution at different $[Cl^-]_{ext}$ (Fig. 8 *D*) is progressively smaller at higher $[Cl^-]_{ext}$ compared to 0 mM and is reduced to <30% at 30 mM $[Cl^-]_{ext}$. The voltage of half-maximal activation of WT at $[Cl^-]_{ext} \leq$ 3 mM is >100 mV (Fig. 8 *F*), similar to what is seen for the mutant E268A (Fig. 3), but much more positive than those of mutant E211D (Fig. 4).

DISCUSSION

In this study, we took advantage of the transient currents elicited by WT and mutant ClC-5 to obtain insight into the molecular mechanism of voltage-sensing of this transporter. Before discussing molecular details that may underlie the capacitive currents, it is important to understand the basic origin of the charge movement. In fact, based on noise analysis and nucleotide regulation it has been suggested that ClC-5 is a gated transporter that undergoes transitions between an inactive state and an active, transporting state (24,31). Such transporter gating has recently been clearly demonstrated for the lysosomal Cl^-/H^+ antiporter ClC-7 (10). Thus, in principle, the observed transient currents might originate either from the gating transitions between inactive and active transporters or from electrogenic steps in the transport cycle.

Although we have extensively studied the effects of Cl^- and H^+ on the transient currents, we cannot definitely discriminate between these two possibilities. It might be that the gating transitions of ClC-5 between the inactive and active states are the underlying basis for the transient currents seen in the E268A mutant. However, in this case it is not clear why the transient currents seen with WT ClC-5 would become larger at low $[Cl^-]_{ext}$. In particular the inward transient currents at negative voltages should be preserved at high $[Cl^-]_{ext}$ and not reduced. On the other hand, it is a well-known conundrum of CLC proteins that gating and ion permeation are strictly interwoven (32–34). Thus, it might be possible that modulation of CLC-5 by Cl^- and H^+ in an unknown way can generate the counterintuitive Cl^- dependence for the transient currents.

The alternative interpretation, that the transient currents reflect electrogenic steps of the transport cycle, would explain their strong decrease in high $[Cl^-]_{ext}$ similar to what is seen for example in the Na-K ATPase. In this pump, the absence of extracellular K^+ impedes the completion of the transport cycle and confines the enzyme to conformational states of the Na^+ translocation branch (32,33).

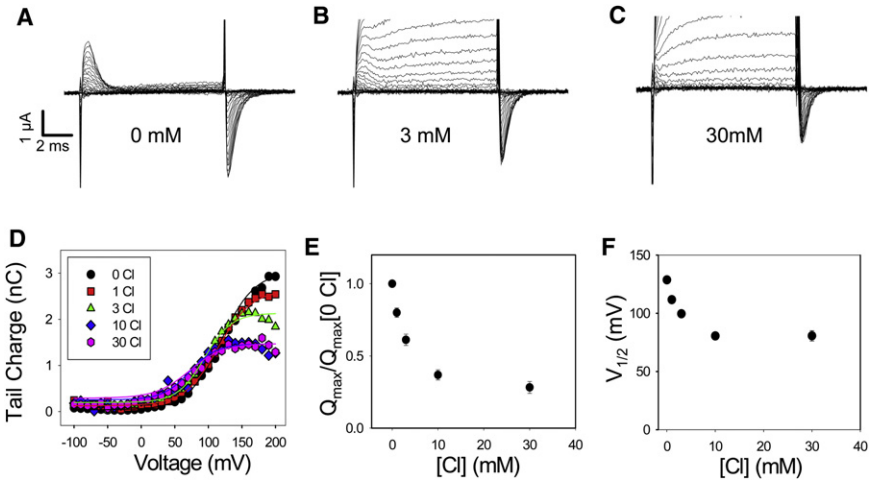

FIGURE 8 Transient currents of WT ClC-5. (*A–C*) Voltage-clamp recordings from an oocyte expressing WT ClC-5 at 0, 3, and 30 mM $[Cl^-]_{ext}$, respectively. Voltage steps ranged from +200 to −120 mV. P/−4 pulses were delivered from a holding potential of −60 mV. Positive currents are out of scale in panels *B* and *C*. (*D*) *Q*(*V*)-relationships at 0, 1, 3, 10, and 30 mM $[Cl^-]_{ext}$ for the same oocyte shown in panels *A–C* superimposed with fits of Eq. 1. Average values are shown for normalized Q_{max} (*E*) and $V_{1/2}$ (*F*) as a function of $[Cl^-]_{ext}$. Error bars indicate mean ± SE ($n \geq 16$).

However, this interpretation is not without problems. In particular, based on noise analysis, a turnover of WT ClC-5 of ~10^5 cycles/s has been reported at large positive voltages (24,31,34), corresponding to a turnover time of ~10 μs. On the other hand, Smith and Lippiat (27) reported time constants of transient currents of E268A ranging from 80 to 500 μs, i.e., at least one-order-of-magnitude slower than the transport cycle of the WT. Even though the noise analysis might have overestimated the turnover rate and the whole-cell patch-clamp kinetic analysis might have underestimated the speed of the transient currents, these data are not easy to reconcile, because partial reactions (in the direction of transport) cannot be slower than overall transport of a full cycle. However, it cannot be excluded, for example, that the mutant E268A, while qualitatively preserving charge-generating transport-related reactions, has slower kinetics than WT ClC-5. Furthermore, even though WT ClC-5 possibly exhibits a fast turnover at high external $[Cl^-]$, transient currents become visible only at low $[Cl^-]_{ext}$, at which turnover is expected to be at least 10-fold slower, being thus qualitatively compatible with the kinetics of the transient currents.

The conclusion that the transient currents represent incomplete transporter cycles has also been reached recently by Grieschat and Alekov (35). Within this interpretation, at low $[Cl^-]_{ext}$, most ClC-5 transporters cannot perform a full transport cycle and are therefore restricted to a limited branch of the cycle comprising certain charge translocating steps. Mutant E268A does not detectably mediate stationary transport (24), but gives rise to transient capacitive currents upon voltage-steps (27). Because the mutation affects the putative intracellular proton acceptor (26), it blocks the completion of a full transport cycle because it limits the supply of protons from the intracellular side toward the gating glutamate. In agreement with this idea, the transient currents were found here to be independent of intracellular pH. Importantly, the similarity of the transient currents of WT ClC-5 in low $[Cl^-]_{ext}$ to those of E268A, suggests that the electrogenic steps in the two cases are the same.

Independent of the question of whether the transient currents reflect gating or transport, a major question regarding the transient currents is whether they represent the movement of a protein-intrinsic voltage sensor, of a substrate Cl^- ion, of a substrate proton (from the outside), or a combination of these.

We found that the transient currents are modulated by pH_{ext}. However, the nature of the modulation (both of E268A as well as E211D) excludes that the transient currents are directly generated by proton-binding/unbinding events. In fact, lowering $[H^+]_{ext}$ to 1 nM did not reduce in any manner the inward transient currents, and lowering $[H^+]_{ext}$ resulted in a leftward shift of the Q-V relationship, opposite to what would be expected if proton movement directly underlies the transients. The molecular substrate of the pH_{ext} modulation remains to be identified.

Regarding the modulation of the transient currents by pH_{ext}, it is interesting to note that this effect appears qualitatively similar to the inhibition of stationary current of ClC-5 produced by acidic pH (36). According to the speculative model we propose here, this similarity might suggest that the conformational changes that originate the transients in the E268A mutant are also critical for the transport activity of WT ClC-5.

As already noted by Smith and Lippiat (27), the transient currents depend on the extracellular anion concentration, but these authors concluded that anion binding/unbinding reactions are not directly involved in the transient currents. Here, we studied the $[Cl^-]_{ext}$ dependence and tested various kinetic models for their compatibility with the data. The simplest model in excellent quantitative agreement with the voltage and chloride dependence of the transient currents is given by Model III in which a conformational change is followed by the binding of Cl^- from the outside. The model predicts a relatively large voltage dependence of

the conformational change (z_C ~ 1.1) and of the subsequent Cl^- binding step (z_K ~ 0.85). Thus, Cl^- binding from the outside contributes to the charge translocation but is not essential.

The Cl^- binding step is associated with a relatively low affinity (K_D(0 mV) ~ 0.8 M). This is in apparent contrast with binding measurements from Picollo et al. (37), who measured a Cl^- binding affinity of ~1 mM in the bacterial ClC-ec1. It has to be stressed, however, that our estimate of the binding affinity is rather indirect and may not represent a true affinity. Furthermore, the measurements of Picollo et al. were performed in nonoriented, detergent-solubilized proteins. In addition, it may also be that there are quantitative differences in the ion-binding properties between ClC-ec1 and ClC-5. This might also be related to the quite different phenotype of the proton glutamate mutation in ClC-ec1, which leads to uncoupled Cl^- transport (26), compared to the transport-deficient mutation E268A in ClC-5. Interestingly, the apparent Cl^- affinity estimated for E268A at large positive voltages (K_D(150 mV) ~ 5 mM) is in the same concentration range at which transient currents become robust in WT ClC-5 (~10 mM).

What is the conformational change that originates the transient currents?

The lack of transient currents of the mutants E211A (27) and E211C/E268A might suggest that a movement of Glu_{ext} itself contributes to the charge displacement currents seen in ClC-5. However, the neutralization of Glu_{ext} alters many qualitative aspects of the transport mechanism. In particular, proton transport is abolished in these mutants but a contribution of proton movement to the transient currents could not be a priori excluded, and in fact it has been previously proposed that proton movement is involved in voltage dependence of ClC-5 (24) and several CLC-channels (38–40). Here, we could exclude a significant direct involvement of protons in the generation of the transient currents. In addition, using NMR analysis of the bacterial ClC-ec1 Cl^-/H^+ antiporter, Elvington et al. (41) described transport-related conformational changes involving a subunit-interface tyrosine residue, which, in principle, could underlie the transient charge movement.

Here, to test more directly the role of Glu_{ext} for the transient currents, we studied the mutation E211D. This mutation abolishes transport but preserves the gating currents, suggesting that Cl^- binding has been either disrupted or is unable to stimulate transport and therefore the gating currents mostly reflect charge movement associated with the conformational changes of the residue at position 211. This is supported by the observation that the midpoint and the steepness of the Q-V relationship are independent of Cl^-_{ext} and that the absolute value of the steepness is roughly the same as z_C for E268A.

Based on the various crystal structures illustrated in the cartoon in Fig. 1, it is tempting to speculate that the conformational change corresponds to the movement of the side chain of the gating glutamate from S_{ext} to S_{cen}. This interpretation is in agreement with the recent crystal structure of a eukaryotic CLC transporter in which the gating glutamate occupies the central anion binding site (25). However, according to Faraldo-Gómez and Roux (42) only 15% of the transmembrane electric field separates S_{ext} and S_{cen}. The apparent voltage-dependence may be larger than anticipated from this by a focusing of the electric field across the membrane and by a contribution from the movement of Cl^- ions bound at S_{cen} that are displaced toward the intracellular space. In agreement with this notion, intracellular Cl^- opposes the charge movement measured in the E268A mutant (27) as well as in the E211D mutant (this work). However, in the absence of more direct structural information, the molecular details of the conformational change remain to be identified.

The transient currents of E211D are dramatically shifted to hyperpolarized potentials and not $[Cl^-]_{ext}$-dependent. Interestingly, the double mutant E211D/E268A had similar properties to the single E211D mutant, suggesting that intracellular protons do not have any influence on the gating currents produced by the aspartate residue. In addition, this result also indirectly supports the notion that alterations of the proton glutamate (E268) do not influence the charge displacement produced by the gating glutamate E211.

How can we rationalize the large shift of the $Q(V)$ relationship of the E211D mutation compared to E268A or WT ClC-5 (at low $[Cl^-]_{ext}$)?

In terms of the cartoon shown in Fig. 1, we can provide a speculative interpretation: At 0 mV, the side chain of a glutamate at position 211 is preferentially in the up-position whereas the aspartate side chain is preferentially in the down-position. Because of this, E211D produces outward transient currents only after applying a conditioning negative prepulse that displaces the aspartate from the down-position to the up-position. In addition, the lack of Cl^- dependence of the $Q(V)$ relationship of E211D suggests that its effective Cl^- affinity is lower compared to that of E268A or WT ClC-5. The smaller effective gating valence of E211D compared with E268A at 100 mM $[Cl^-]_{ext}$ (Fig. 6 *D*) is in agreement with this interpretation.

In general, our data on ClC-5 are probably of relevance for the voltage-dependent gating of CLC channels, for which it has been notoriously difficult to distinguish among Cl^--mediated, proton-mediated, or intrinsic voltage dependence (21,39,40,43–48). In particular, the effect of extracellular Cl^- on the gating charge movement of mutant E268A could be described as an allosteric stabilization of an activated conformation of the gating glutamate in line with the proposal of Miller (38) according to which extracellular Cl^- is an allosteric gating modifier of CLC-channels.

In summary, our results suggest that the molecular events leading to these currents could be an inward movement of the side chain of Glu_{ext}, accompanied by a movement of

a Cl^- ion to the intracellular side, and followed by the binding of an extracellular Cl^- ion.

SUPPORTING MATERIAL

Seven figures are available at http://www.biophysj.org/biophysj/supplemental/S0006-3495(12)00408-0.

We thank Consuelo Murgia and Francesca Quartino for technical assistance.

The financial support by the Italian Institute of Technology (progetto SEED), Telethon Italy (model No. GGP08064), and the Compagnia San Paolo is gratefully acknowledged.

REFERENCES

1. Jentsch, T. J. 2008. CLC chloride channels and transporters: from genes to protein structure, pathology and physiology. *Crit. Rev. Biochem. Mol. Biol.* 43:3–36.
2. Miller, C. 1982. Open-state substructure of single chloride channels from *Torpedo* electroplax. *Philos. Trans. R. Soc. Lond. B Biol. Sci.* 299:401–411.
3. Bauer, C. K., K. Steinmeyer, …, T. J. Jentsch. 1991. Completely functional double-barreled chloride channel expressed from a single *Torpedo* cDNA. *Proc. Natl. Acad. Sci. USA.* 88:11052–11056.
4. Accardi, A., and C. Miller. 2004. Secondary active transport mediated by a prokaryotic homologue of ClC Cl^- channels. *Nature.* 427: 803–807.
5. Picollo, A., and M. Pusch. 2005. Chloride/proton antiporter activity of mammalian CLC proteins ClC-4 and ClC-5. *Nature.* 436:420–423.
6. Scheel, O., A. A. Zdebik, …, T. J. Jentsch. 2005. Voltage-dependent electrogenic chloride/proton exchange by endosomal CLC proteins. *Nature.* 436:424–427.
7. De Angeli, A., D. Monachello, …, H. Barbier-Brygoo. 2006. The nitrate/proton antiporter AtCLCa mediates nitrate accumulation in plant vacuoles. *Nature.* 442:939–942.
8. Graves, A. R., P. K. Curran, …, J. A. Mindell. 2008. The Cl^-/H^+ antiporter ClC-7 is the primary chloride permeation pathway in lysosomes. *Nature.* 453:788–792.
9. Neagoe, I., T. Stauber, …, T. J. Jentsch. 2010. The late endosomal ClC-6 mediates proton/chloride countertransport in heterologous plasma membrane expression. *J. Biol. Chem.* 285:21689–21697.
10. Leisle, L., C. F. Ludwig, …, T. Stauber. 2011. ClC-7 is a slowly voltage-gated $2Cl^-/1H^+$-exchanger and requires OstM1 for transport activity. *EMBO J.* 30:2140–2152.
11. Zifarelli, G., and M. Pusch. 2007. CLC chloride channels and transporters: a biophysical and physiological perspective. *Rev. Physiol. Biochem. Pharmacol.* 158:23–76.
12. Novarino, G., S. Weinert, …, T. J. Jentsch. 2010. Endosomal chloride-proton exchange rather than chloride conductance is crucial for renal endocytosis. *Science.* 328:1398–1401.
13. Weinert, S., S. Jabs, …, T. J. Jentsch. 2010. Lysosomal pathology and osteopetrosis upon loss of H^+-driven lysosomal Cl^- accumulation. *Science.* 328:1401–1403.
14. Lloyd, S. E., S. H. Pearce, …, R. V. Thakker. 1996. A common molecular basis for three inherited kidney stone diseases. *Nature.* 379:445–449.
15. Günther, W., N. Piwon, and T. J. Jentsch. 2003. The ClC-5 chloride channel knock-out mouse—an animal model for Dent's disease. *Pflugers Arch.* 445:456–462.
16. Piwon, N., W. Günther, …, T. J. Jentsch. 2000. ClC-5 Cl^--channel disruption impairs endocytosis in a mouse model for Dent's disease. *Nature.* 408:369–373.
17. Wang, S. S., O. Devuyst, …, W. B. Guggino. 2000. Mice lacking renal chloride channel, CLC-5, are a model for Dent's disease, a nephrolithiasis disorder associated with defective receptor-mediated endocytosis. *Hum. Mol. Genet.* 9:2937–2945.
18. Maritzen, T., G. Rickheit, …, T. J. Jentsch. 2006. Kidney-specific upregulation of vitamin D3 target genes in ClC-5 KO mice. *Kidney Int.* 70:79–87.
19. Steinmeyer, K., B. Schwappach, …, T. J. Jentsch. 1995. Cloning and functional expression of rat CLC-5, a chloride channel related to kidney disease. *J. Biol. Chem.* 270:31172–31177.
20. Bezanilla, F. 2008. How membrane proteins sense voltage. *Nat. Rev. Mol. Cell Biol.* 9:323–332.
21. Zifarelli, G., and M. Pusch. 2010. The role of protons in fast and slow gating of the *Torpedo* chloride channel ClC-0. *Eur. Biophys. J.* 39:869–875.
22. Dutzler, R., E. B. Campbell, …, R. MacKinnon. 2002. X-ray structure of a ClC chloride channel at 3.0 Å reveals the molecular basis of anion selectivity. *Nature.* 415:287–294.
23. Dutzler, R., E. B. Campbell, and R. MacKinnon. 2003. Gating the selectivity filter in ClC chloride channels. *Science.* 300:108–112.
24. Zdebik, A. A., G. Zifarelli, …, M. Pusch. 2008. Determinants of anion-proton coupling in mammalian endosomal CLC proteins. *J. Biol. Chem.* 283:4219–4227.
25. Feng, L., E. B. Campbell, …, R. MacKinnon. 2010. Structure of a eukaryotic CLC transporter defines an intermediate state in the transport cycle. *Science.* 330:635–641.
26. Accardi, A., M. Walden, …, C. Miller. 2005. Separate ion pathways in a Cl^-/H^+ exchanger. *J. Gen. Physiol.* 126:563–570.
27. Smith, A. J., and J. D. Lippiat. 2010. Voltage-dependent charge movement associated with activation of the CLC-5 $2Cl^-/1H^+$ exchanger. *FASEB J.* 24:3696–3705.
28. Jurman, M. E., L. M. Boland, …, G. Yellen. 1994. Visual identification of individual transfected cells for electrophysiology using antibody-coated beads. *Biotechniques.* 17:876–881.
29. Hamill, O. P., A. Marty, …, F. J. Sigworth. 1981. Improved patch-clamp techniques for high-resolution current recording from cells and cell-free membrane patches. *Pflugers Arch.* 391:85–100.
30. Kapus, A., R. Romanek, …, S. Grinstein. 1993. A pH-sensitive and voltage-dependent proton conductance in the plasma membrane of macrophages. *J. Gen. Physiol.* 102:729–760.
31. Zifarelli, G., and M. Pusch. 2009. Intracellular regulation of human ClC-5 by adenine nucleotides. *EMBO Rep.* 10:1111–1116.
32. Nakao, M., and D. C. Gadsby. 1986. Voltage dependence of Na translocation by the Na/K pump. *Nature.* 323:628–630.
33. De Weer, P., D. C. Gadsby, and R. F. Rakowski. 1988. Voltage dependence of the Na-K pump. *Annu. Rev. Physiol.* 50:225–241.
34. Zifarelli, G., and M. Pusch. 2009. Conversion of the $2Cl^-/1H^+$ + antiporter ClC-5 in a NO_3^-/H+ antiporter by a single point mutation. *EMBO J.* 28:175–182.
35. Grieschat, M., and A. K. Alekov. 2012. Glutamate 268 regulates transport probability of the anion/proton exchanger CIC-5. *J. Biol. Chem.* 287:8101–8109.
36. Picollo, A., M. Malvezzi, and A. Accardi. 2010. Proton block of the CLC-5 Cl^-/H^+ exchanger. *J. Gen. Physiol.* 135:653–659.
37. Picollo, A., M. Malvezzi, …, A. Accardi. 2009. Basis of substrate binding and conservation of selectivity in the CLC family of channels and transporters. *Nat. Struct. Mol. Biol.* 16:1294–1301.
38. Miller, C. 2006. ClC chloride channels viewed through a transporter lens. *Nature.* 440:484–489.
39. Zifarelli, G., A. R. Murgia, …, M. Pusch. 2008. Intracellular proton regulation of ClC-0. *J. Gen. Physiol.* 132:185–198.
40. Niemeyer, M. I., L. P. Cid, …, F. V. Sepúlveda. 2009. Voltage-dependent and -independent titration of specific residues accounts for complex gating of a ClC chloride channel by extracellular protons. *J. Physiol.* 587:1387–1400.

41. Elvington, S. M., C. W. Liu, and M. C. Maduke. 2009. Substrate-driven conformational changes in ClC-ec1 observed by fluorine NMR. *EMBO J.* 28:3090–3102.

42. Faraldo-Gómez, J. D., and B. Roux. 2004. Electrostatics of ion stabilization in a ClC chloride channel homologue from *Escherichia coli*. *J. Mol. Biol.* 339:981–1000.

43. Pusch, M., U. Ludewig, …, T. J. Jentsch. 1995. Gating of the voltage-dependent chloride channel CIC-0 by the permeant anion. *Nature.* 373:527–531.

44. Chen, T. Y., and C. Miller. 1996. Nonequilibrium gating and voltage dependence of the ClC-0 Cl^- channel. *J. Gen. Physiol.* 108:237–250.

45. Chen, M. F., and T. Y. Chen. 2001. Different fast-gate regulation by external Cl^- and H^+ of the muscle-type ClC chloride channels. *J. Gen. Physiol.* 118:23–32.

46. Traverso, S., G. Zifarelli, …, M. Pusch. 2006. Proton sensing of CLC-0 mutant E166D. *J. Gen. Physiol.* 127:51–65.

47. Engh, A. M., J. D. Faraldo-Gómez, and M. Maduke. 2007. The mechanism of fast-gate opening in ClC-0. *J. Gen. Physiol.* 130:335–349.

48. Sánchez-Rodríguez, J. E., J. A. De Santiago-Castillo, and J. Arreola. 2010. Permeant anions contribute to voltage dependence of ClC-2 chloride channel by interacting with the protopore gate. *J. Physiol.* 588:2545–2556.